Supporting Information

Temperature-Responsive Molecular Liquids Based on Dihydrophenazines for Dynamic Multicolor-Fluorescent Anti-Counterfeiting and Encryption

Hao Liu,[a] *Wenxuan Song,*[a] *Xuanying Chen,*[a] *Ju Mei,**[a] *Zhiyun Zhang,**[a] *and Jianhua Su*[a]

[a] Key Laboratory for Advanced Materials, Feringa Nobel Prize Scientist Joint Research Center, Institute of Fine Chemicals, Joint International Research Laboratory for Precision Chemistry and Molecular Engineering, School of Chemistry and Molecular Engineering, East China University of Science & Technology, 130 Meilong Road, Shanghai, 200237, China

Table S1. Relative abilities of the currently available "similar" anticounterfeiting and encryption materials.

Sources	Materials	Abilities/Properties
This work	Temperature-responsive molecular liquids based on dual-emissive organic fluorogens	i) Temperature-dependent dynamic multicolor-fluorescent outputs; ii) Higher-level product security against counterfeiting; iii) Excellent reversibility and repeatability; iv) Simple preparation process; v) Solvent-free, dopant-free, and hence environment friendly; vi) Multi-modal anti-counterfeiting; vii) No requirement for complex encoding-decoding instrumentation
Ref 26	Mn^{2+}-doped nanoparticles	i) Multilevel anti-counterfeiting with high-throughput rate; ii) Binary temporal codes generation for efficient data encoding; iii) Without the need for complex time-gated decoding instrumentation
Ref S1	Photoswitchable fluorescent liquid crystal polymeric nanoparticles	i) Aggregation-induced emission enhancement feature; ii) Water-dispersible; iii) High contrast; iv) Good repeatability
Ref 34	Graphene quantum dots	i) Environment friendliness; ii) Low cost; iii) Easy preparation; iv) Order-sensitive stimulus-responsive information encryption
Ref S2	Lanthanide-doped nanoparticles	i) Readily deposited or patterned as films to create multicolor barcodes; ii) Flexibility in high-density data storage; iii) Multidimensional information memory

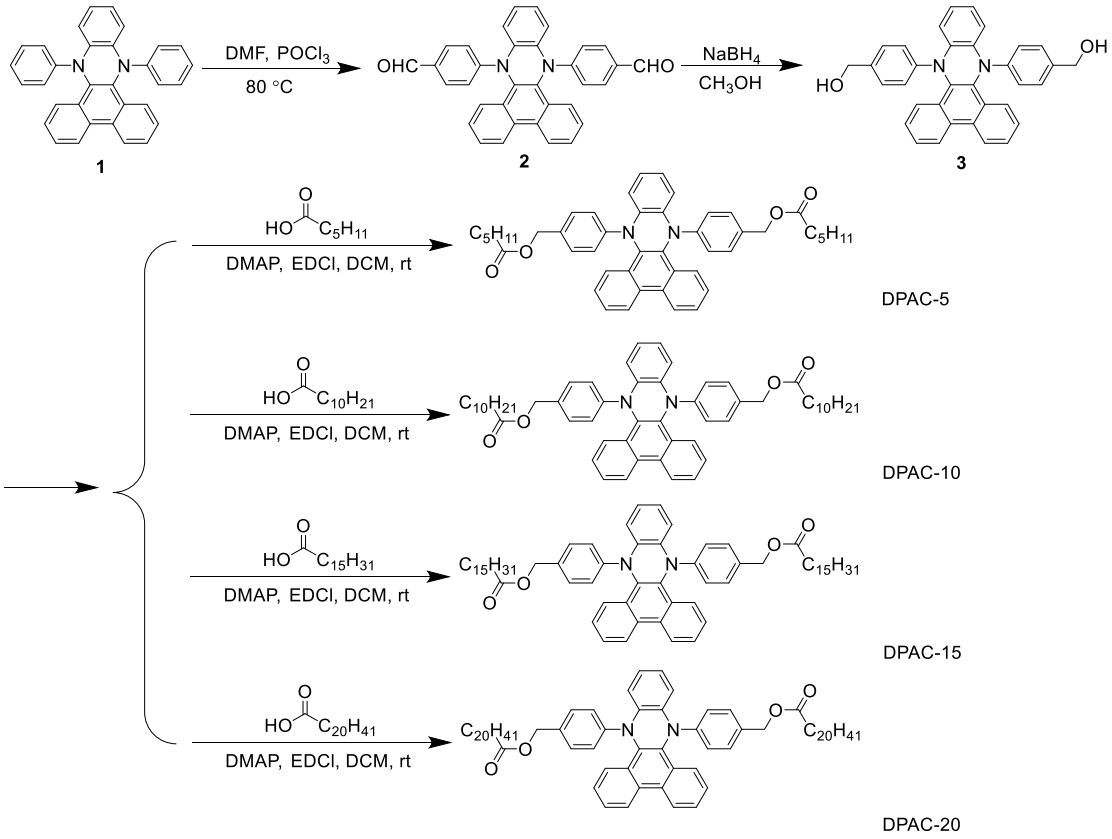

Scheme S1. Synthetic route to DPAC-5, DPAC-10, DPAC-15, and DPAC-20.

The original spectra

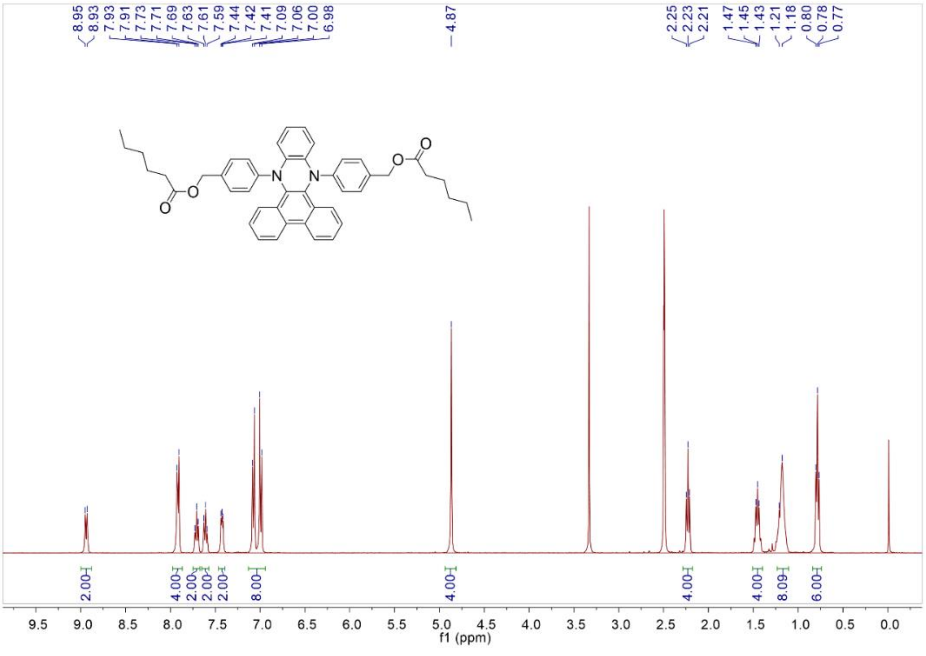

Figure S1. ^{1}H NMR spectrum of DPAC-5 in DMSO-d_6.

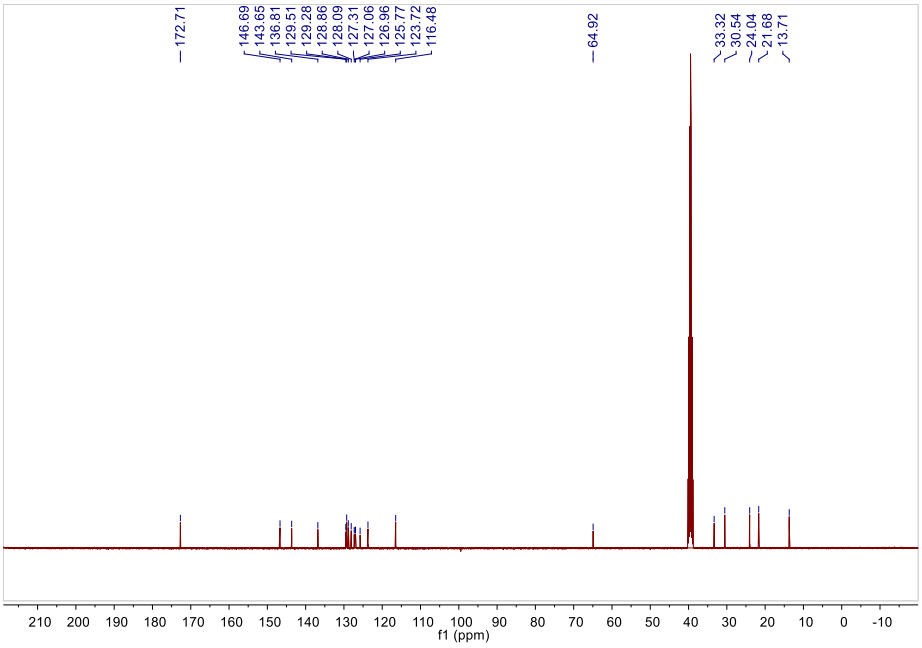

Figure S2. ^{13}C NMR spectrum of DPAC-5 in DMSO-d_6.

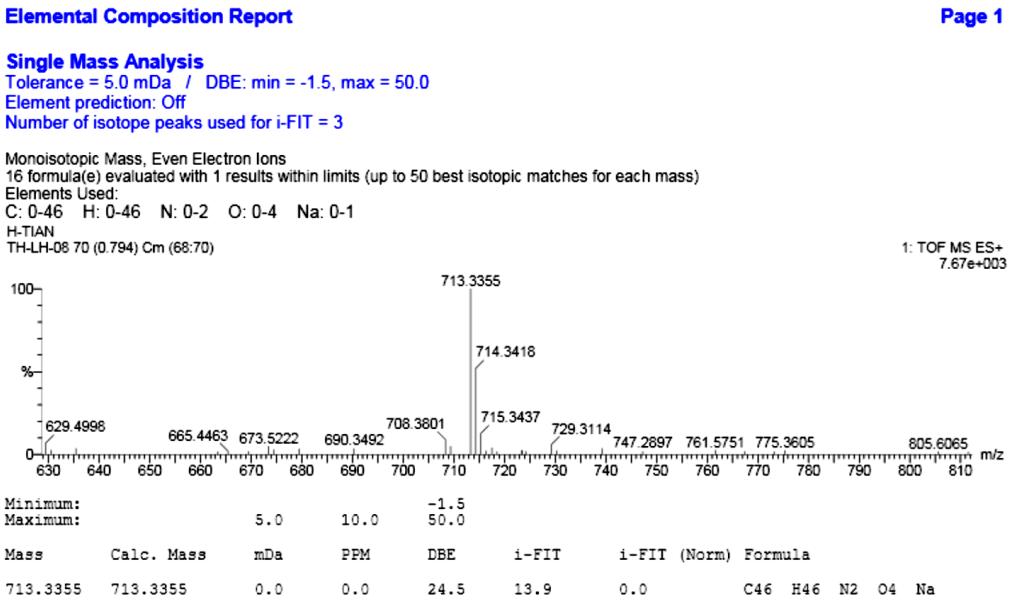

Figure S3. HRMS spectrum of DPAC-5.

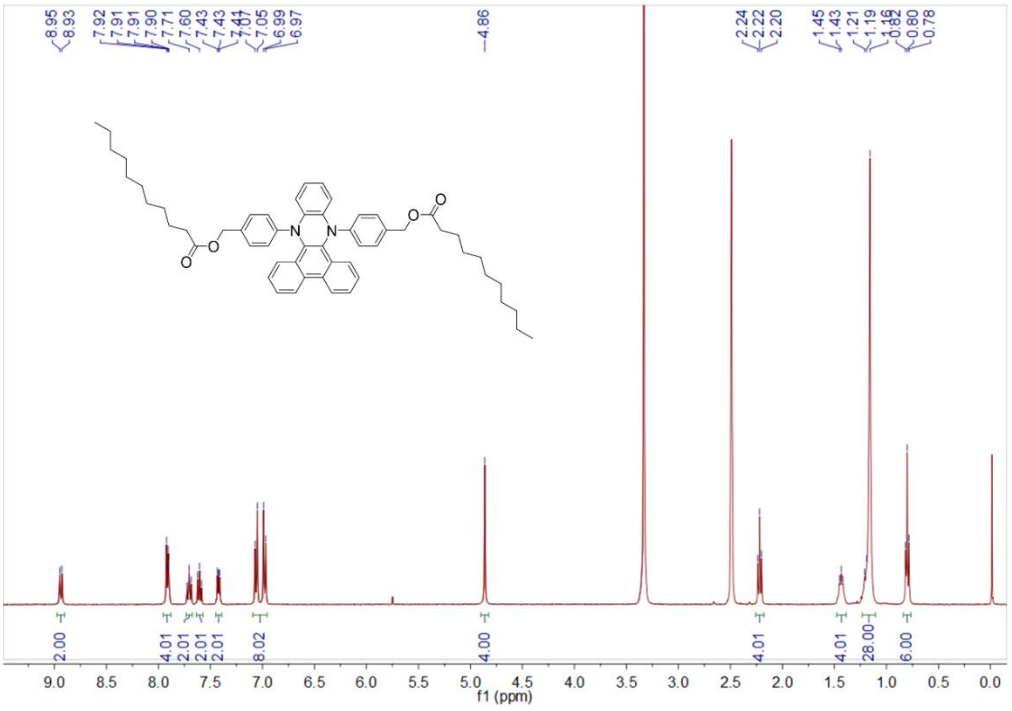

Figure S4. ^{1}H NMR spectrum of DPAC-10 in DMSO-d_6.

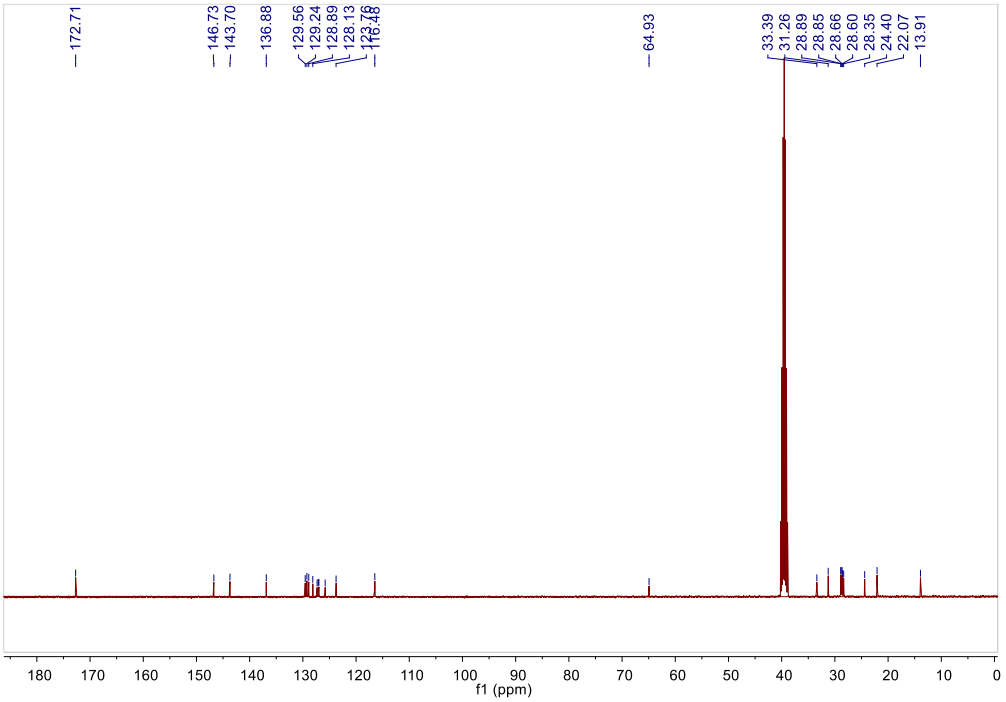

Figure S5. ^{13}C NMR spectrum of DPAC-10 in DMSO-d_6.

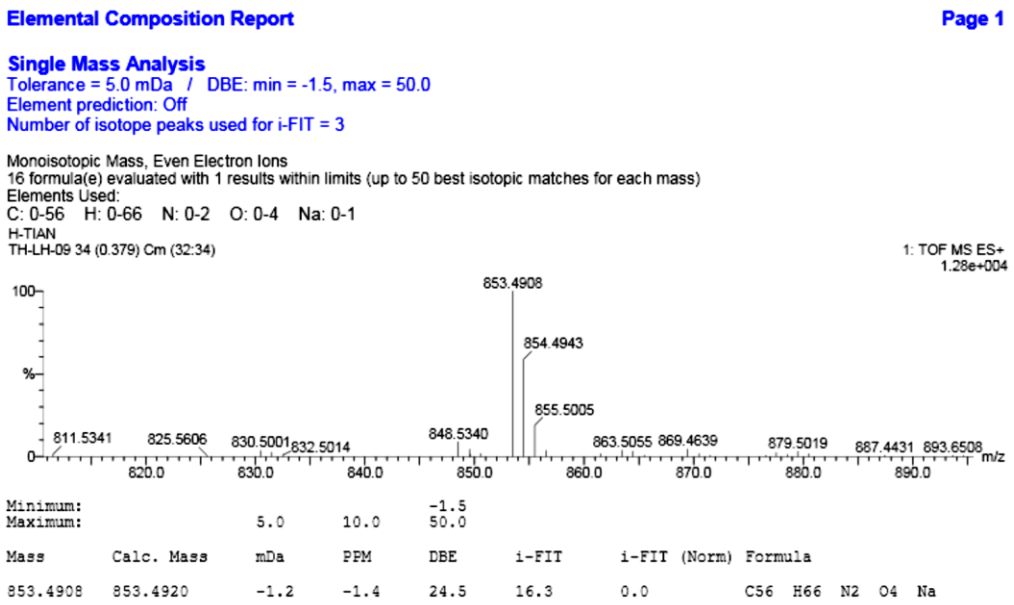

Figure S6. HRMS spectrum of DPAC-10.

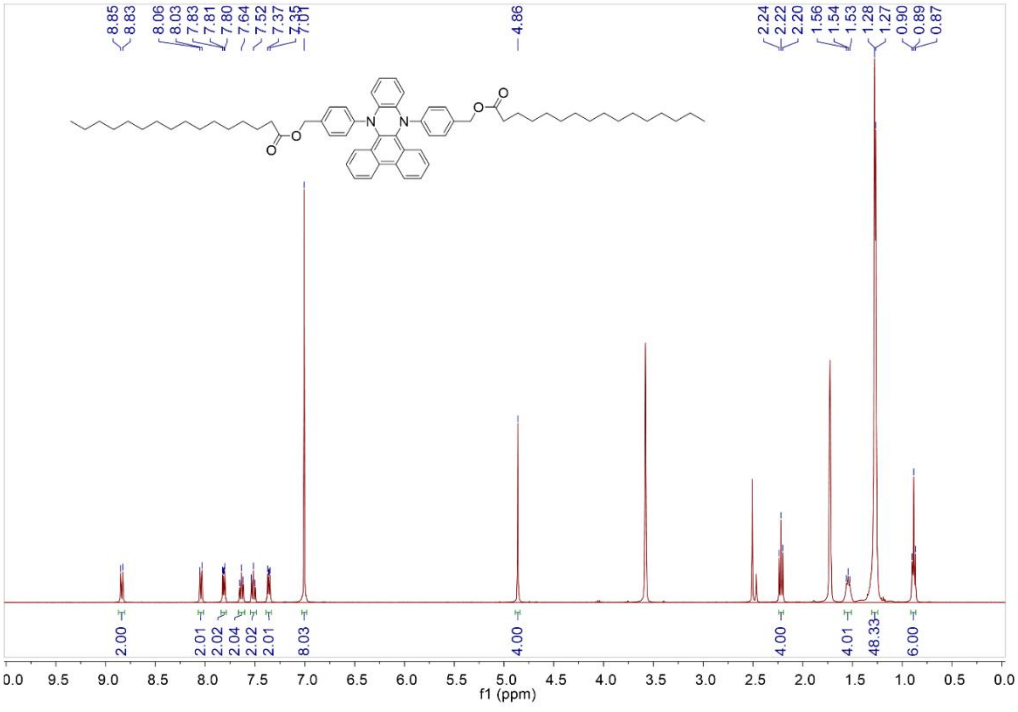

Figure S7. ^{1}H NMR spectrum of DPAC-15 in THF-d_8.

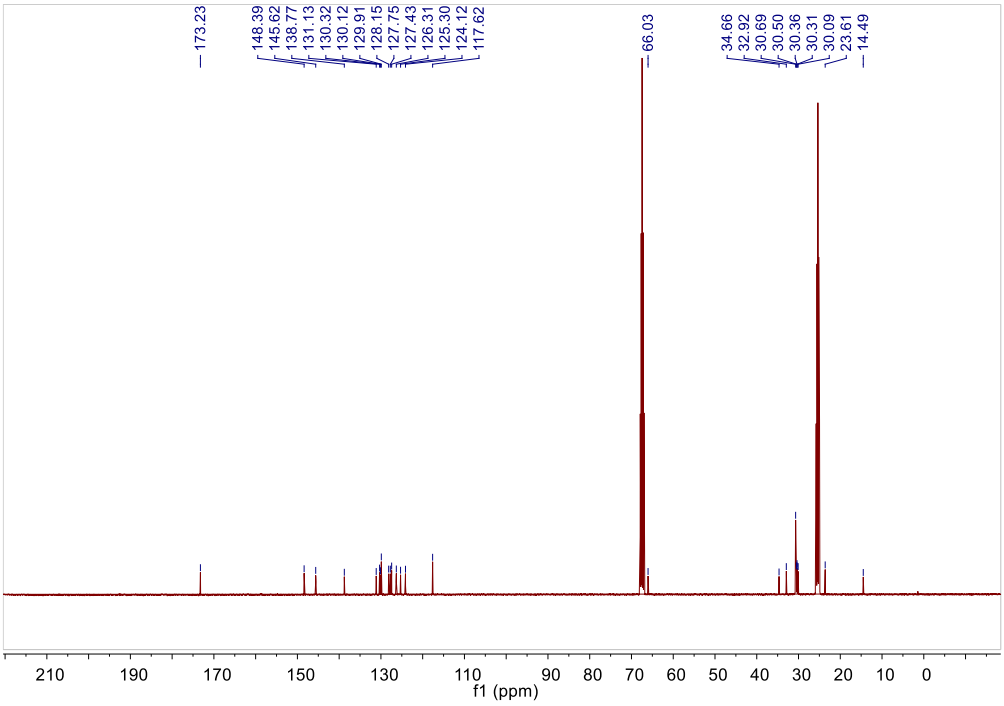

Figure S8. ^{13}C NMR spectrum of DPAC-15 in THF-d_8.

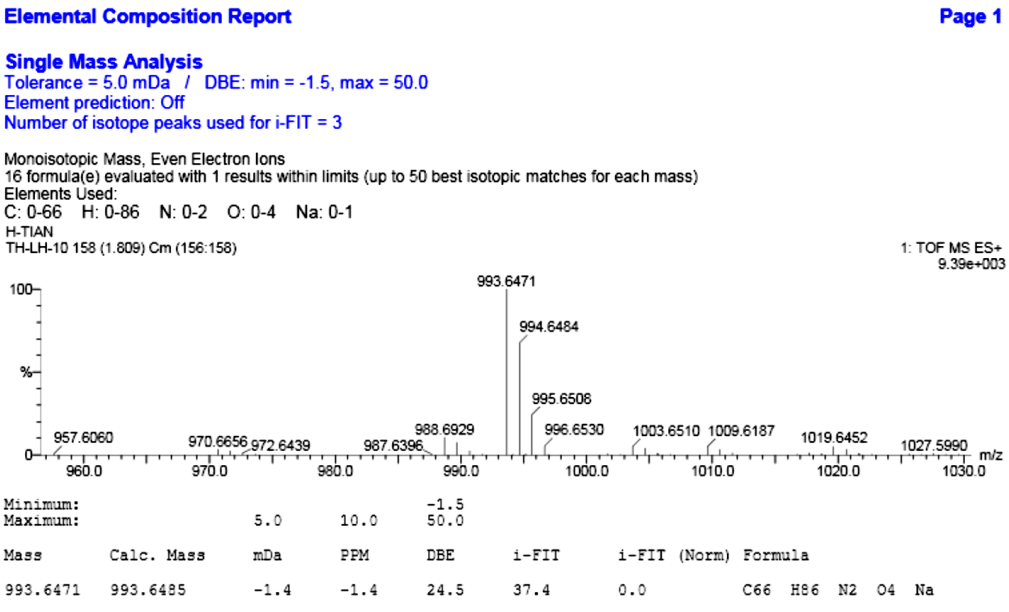

Figure S9. HRMS spectrum of DPAC-15.

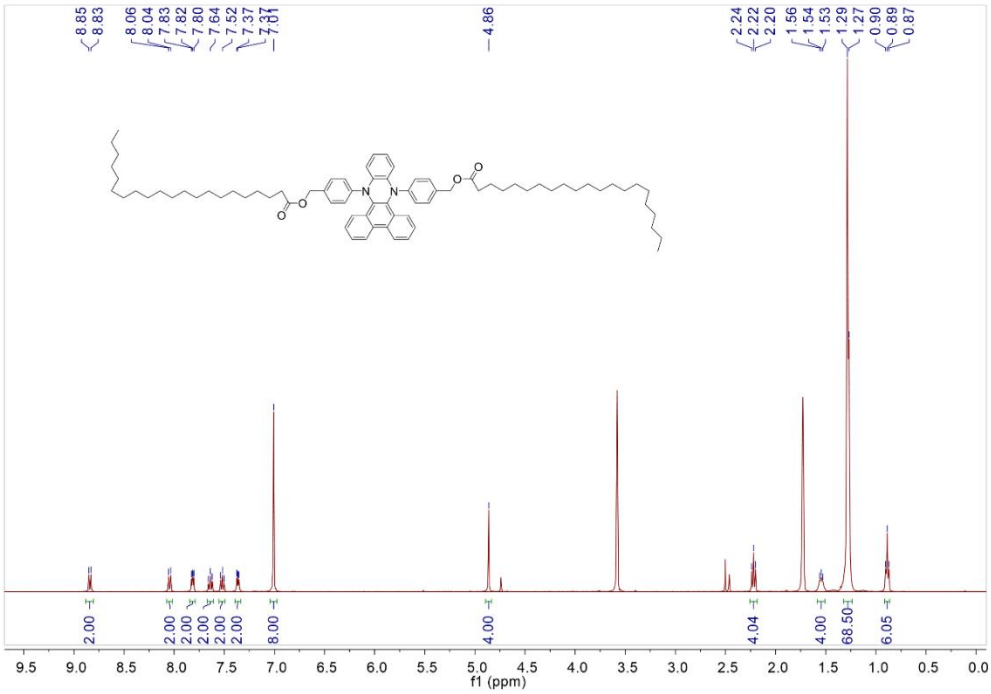

Figure S10. ^{1}H NMR spectrum of DPAC-20 in THF-d_8.

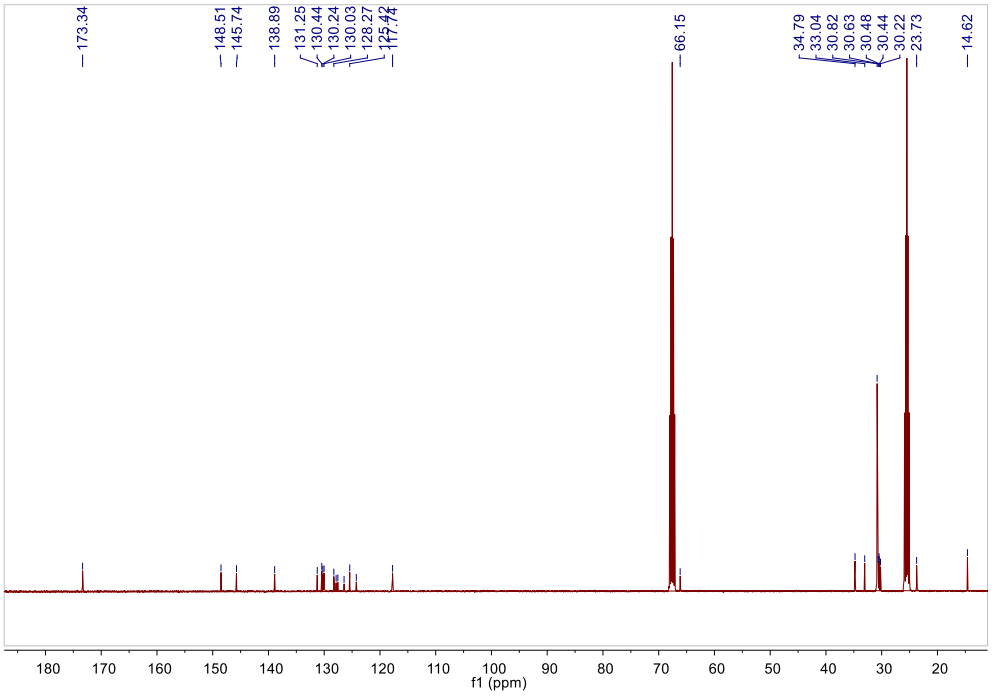

Figure S11. ^{13}C NMR spectrum of DPAC-20 in THF-d_8.

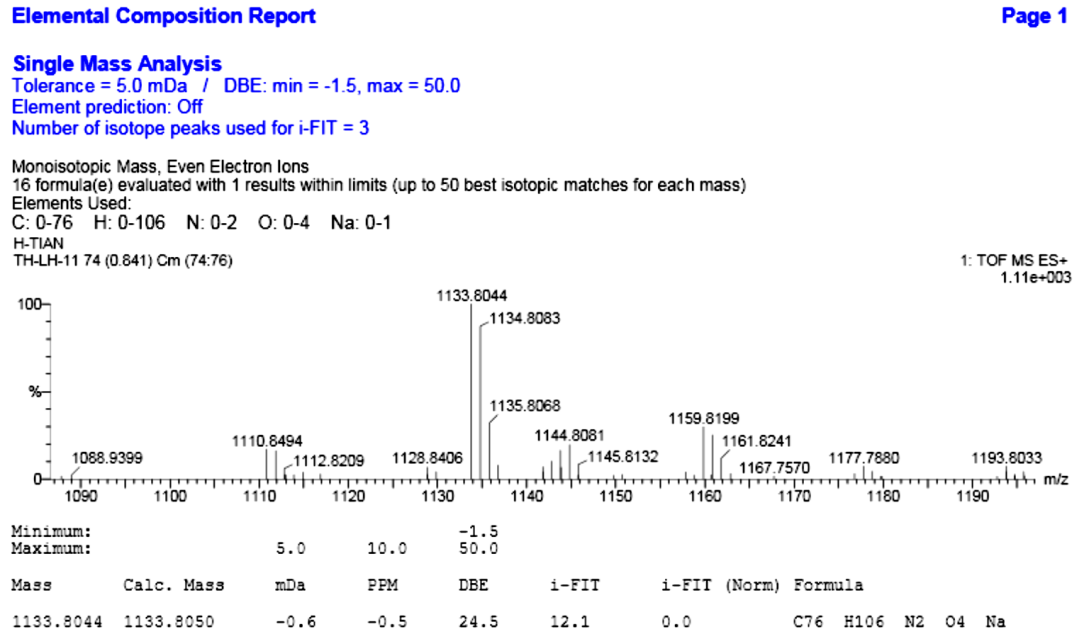

Figure S12. HRMS spectrum of DPAC-20.

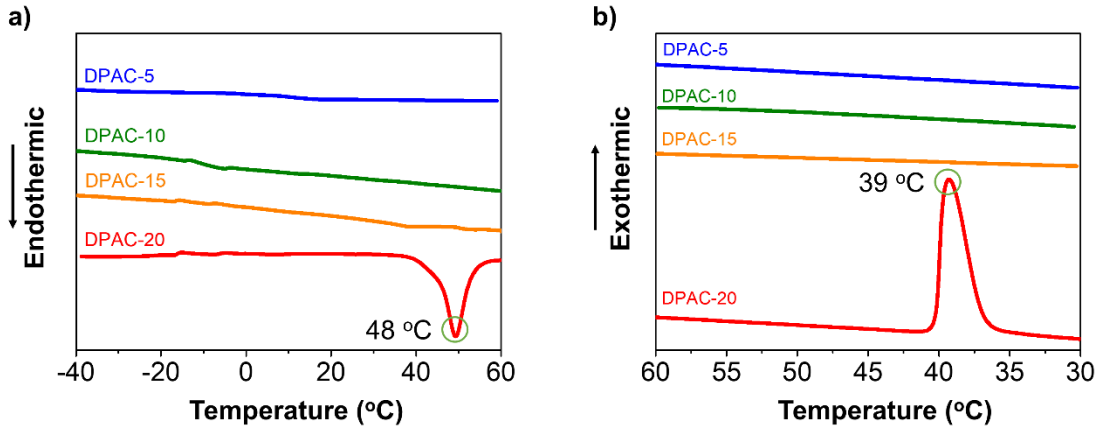

Figure S13. DSC thermograms of the DPAC-*n* compounds in the a) heating and b) cooling courses.

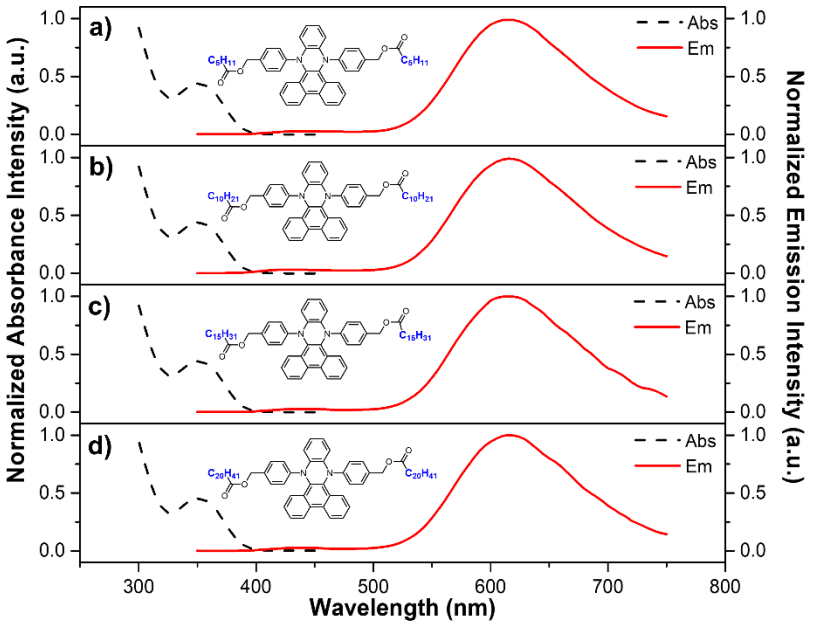

Figure S14. Absorption (black lines) and emission (red lines) spectra of (a) DPAC-5, (b) DPAC-10, (c) DPAC-15, and (d) DPAC-20 in dichloromethane (10^{-5} M) (excited at 365 nm).

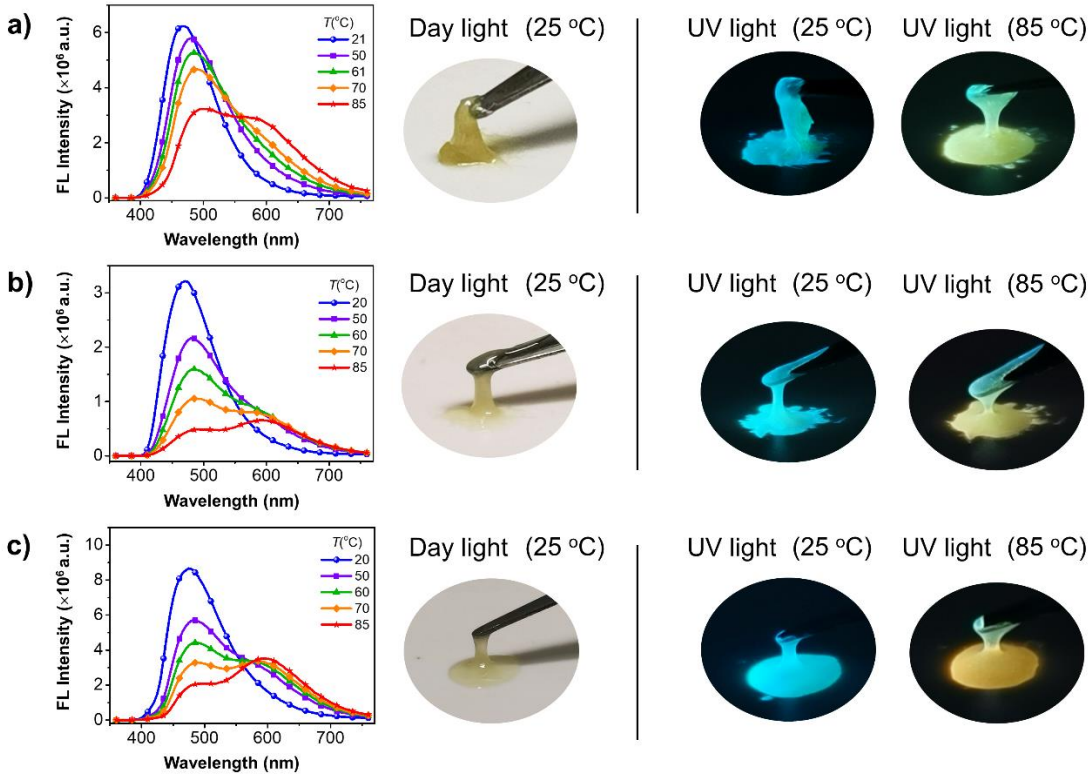

Figure S15. Fluorescence spectra of DPAC-*n* derivatives when the temperature varies from 20 to 85 °C, and the images under the daylight (left) at 25 °C and 365 nm UV light at 25 °C (middle) and 85 °C (right) of the solvent-free liquids of a) DPAC-5, b) DPAC-10, and c) DPAC-15.

Table S2. Quantum yields of four compounds at 20 ºC, and 85 ºC.

Temperature	Quantum yield (%)			
	DPAC-5	DPAC-10	DPAC-15	DPAC-20
20 ºC	77.8	80.1	81.4	82.2
85 ºC	61.9	54.4	52.4	45.3

Note: The fluorescence quantum yields of all the DPAC-*n* derivatives were tested using HAMAMATSU Quantaurus-QY C11347-11. Since the instrument for the measurement of fluorescence quantum yields cannot directly heat samples, we heated the samples using an external heater. Each sample was heated to 85 ºC and kept at this temperature for 10 minutes, and afterwards was quickly put into the sample cell of HAMAMATSU Quantaurus-QY C11347-11 for testing. The fluorescence quantum yields were acquired point by point as the temperature decreased from 85 to 20 ºC. Each measurement was repeated for three times.

Table S3. CIE coordinates of DPAC-*n* from 20 ºC to 85 ºC

	CIE coordinates (*x*, *y*)			
T (ºC)	DPAC-5	DPAC-10	DPAC-15	DPAC-20
20	(0.18, 0.24)	(0.18, 0.25)	(0.21, 0.30)	(0.18, 0.24)
25	(0.19, 0.25)	(0.19, 0.26)	/	/
30	(0.19, 0.27)	(0.20, 0.28)	(0.23, 0.32)	(0.19, 0.26)
35	(0.20, 0.28)	(0.21, 0.30)	(0.25, 0.34)	/
49	(0.21, 0.30)	(0.23, 0.31)	(0.26, 0.35)	(0.20, 0.27)
45	(0.22, 0.31)	(0.24, 0.33)	(0.27, 0.36)	(0.26, 0.34)
50	(0.23, 0.33)	(0.25, 0.34)	(0.29, 0.37)	(0.32, 0.38)
55	(0.24, 0.34)	(0.27, 0.35)	(0.30, 0.38)	(0.34, 0.39)
60	(0.26, 0.36)	(0.29, 0.37)	(0.33, 0.39)	(0.36, 0.40)
65	(0.27, 0.37)	(0.31, 0.38)	(0.34, 0.40)	(0.38, 0.41)
70	(0.28, 0.38)	(0.32, 0.38)	(0.36, 0.41)	(0.40, 0.41)
75	(0.30, 0.40)	(0.34, 0.39)	(0.38, 0.41)	(0.42, 0.42)
80	(0.32, 0.41)	(0.36, 0.40)	/	(0.43, 0.42)
85	(0.35, 0.42)	(0.39, 0.41)	(0.42, 0.42)	(0.45, 0.43)

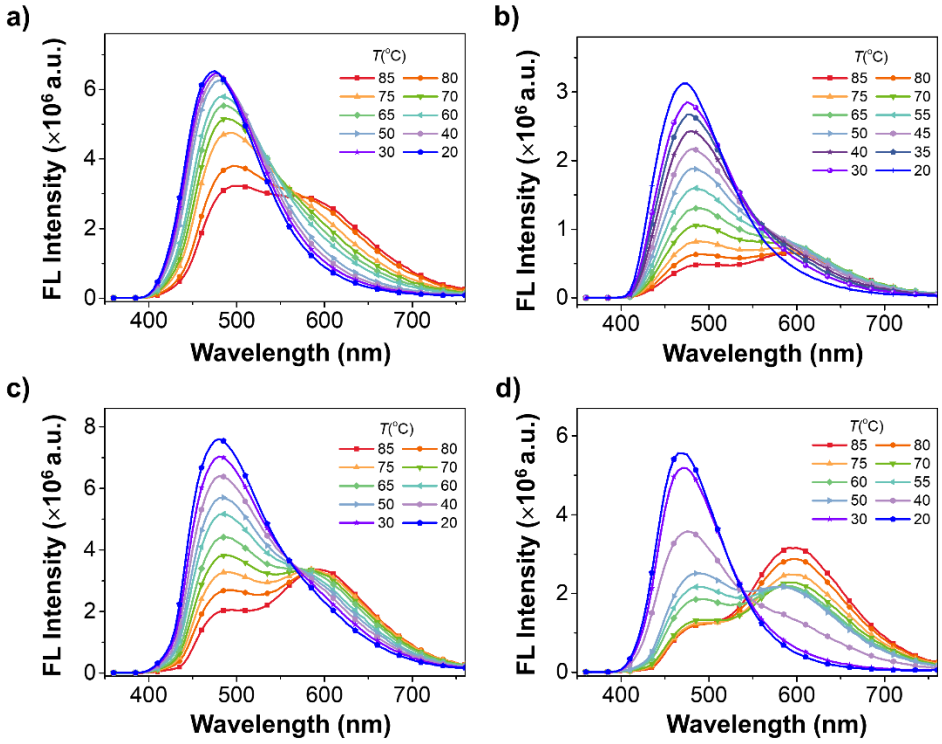

Figure S16. Fluorescence spectra recorded during the cooling process from 85 ºC to 20 ºC of a) DPAC-5, b) DPAC-10, c) DPAC-15, and d) DPAC-20.

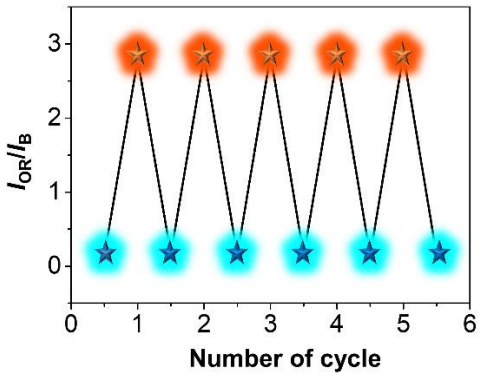

Figure S17. Reversible change in I_{OR}/I_B of DPAC-20 upon cycling the temperature five times between 40 ºC and 85 ºC. The "red stars" stand for the predominate orange-red fluorescence of DPAC-20 at 85 ºC, while the "cyan stars" represent the dominant blue fluorescence at 40 ºC.

S1 J. Li, M. Tian, H. Xu, X. Ding and J. Guo, *Part. Part. Syst. Charact.*, 2019, **36**, 1900346.

S2 X. Li, Y. Xie, B. Song, H. L. Zhang, H. Chen, H. Cai, W. Liu and Y. Tang, *Angew. Chem. Int. Ed.*, 2017, **56**, 2689-2693.